Supporting Information

Confined Growth and Controlled Coalescence/Self-Removal of Condensate Microdrops on Spatially Heterogeneously-Patterned Superhydrophilic-Superhydrophobic Surface

*Dandan Xing[1,2‡], Rui Wang[1,‡], Feifei Wu[1], and Xuefeng Gao[1,2]**

[1] Functional Materials and Interfaces Lab, Suzhou Institute of Nano-Tech and Nano-Bionics, Chinese Academy of Sciences, Suzhou 215123, P. R. China

[2] School of Nano-Tech and Nano-Bionics, University of Science and Technology of China, Hefei 230026, P. R. China

*Corresponding Author: xfgao2007@sinano.ac.cn

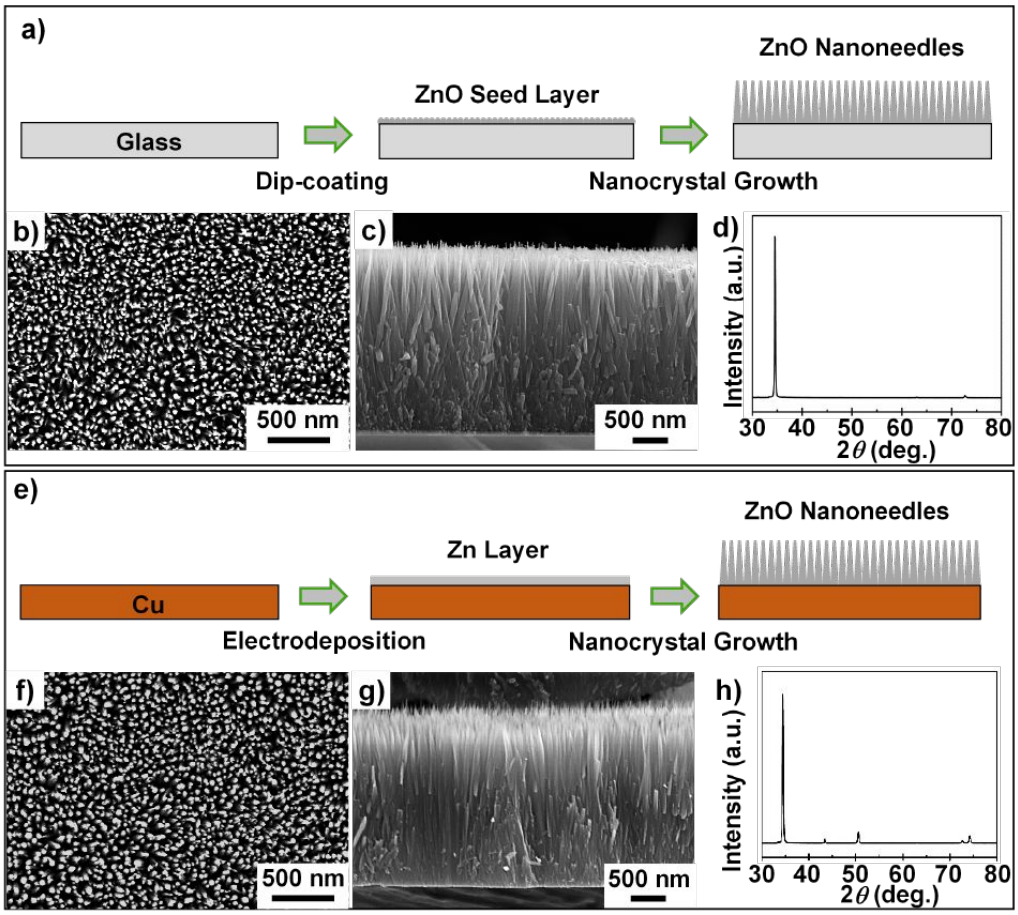

Figure S1. In-situ growth of aligned ZnO nanoneedles on the surface of glass slides (a-d) and copper plates (e-h). a) Schematic showing a two-step fabrication process: first coating ZnO seed layers and then growing nanoneedles on glass surface. b-d) Typical SEM top-view (b), side-view (c) and XRD spectrum (d) of the as-prepared nanoneedles. e) Schematic showing a two-step fabrication process: first electrodepositing Zn seed layers and then growing ZnO nanoneedles on copper surface. f-h) Typical SEM top-view (f), side-view (g) and XRD spectrum (h) of the as-prepared nanoneedles. Here, glass slides are used for the fluorescence imaging of heterogeneous patterns due to their optical transparency, while copper plates are used for condensation experiments of all samples due to their higher thermal conductivity.

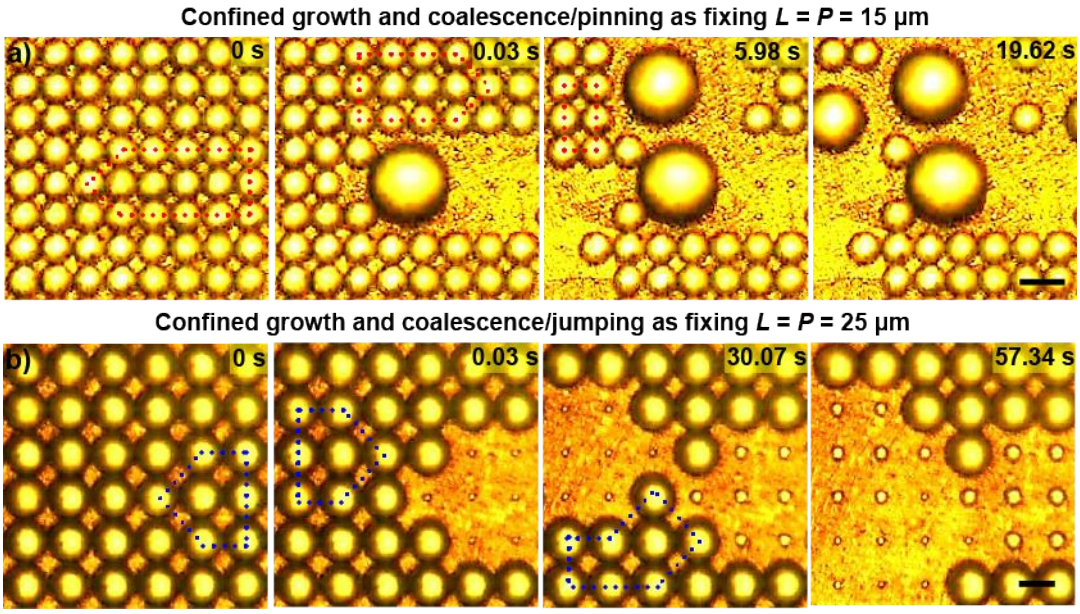

Figure S2. Time-lapse optical images showing distinct condensation behaviors: (a) confined growth and random coalescence/pinning as $L = P = 15$ μm; (b) confined growth and random coalescence/self-ejection as $L = P = 25$ μm. Here, $D = 2$ μm and $N = 4$.

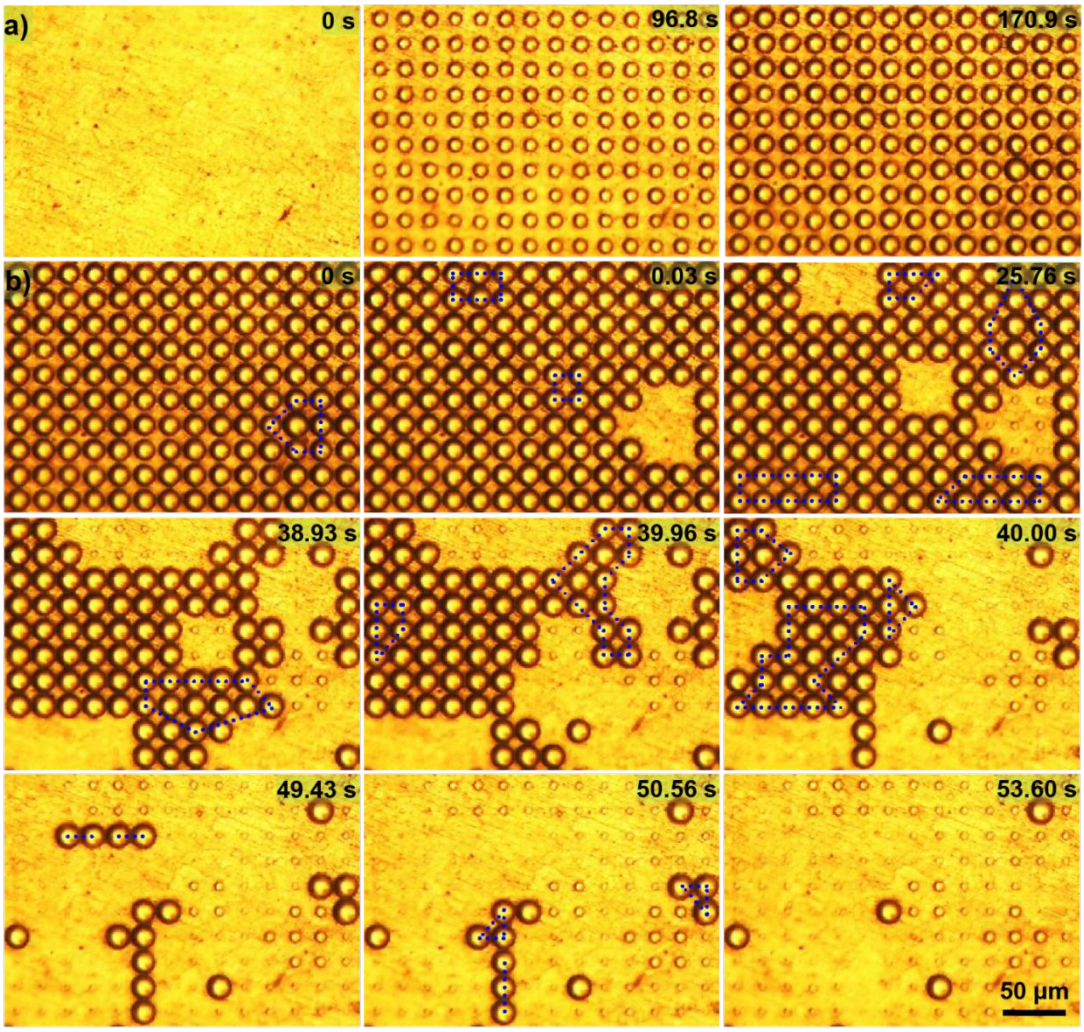

Figure S3. Large-area optical images are given to present the confined growth (a) but uncontrolled coalescence/self-ejection (b) details of condensate microdrops on the homogeneously-patterned surface with $N = 4$, $D = 2$ μm, $L = P = 20$ μm. Here, "0 s" labeling in the panel of **a** and **b** refers to the moment of condensation beginning and the moment before the first coalescence of "in-site" condensate microdrops, respectively. Clearly, such homogeneous pattern cannot simultaneously realize the confined growth and controlled coalescence/self-ejection of "in-site" condensate microdrops.

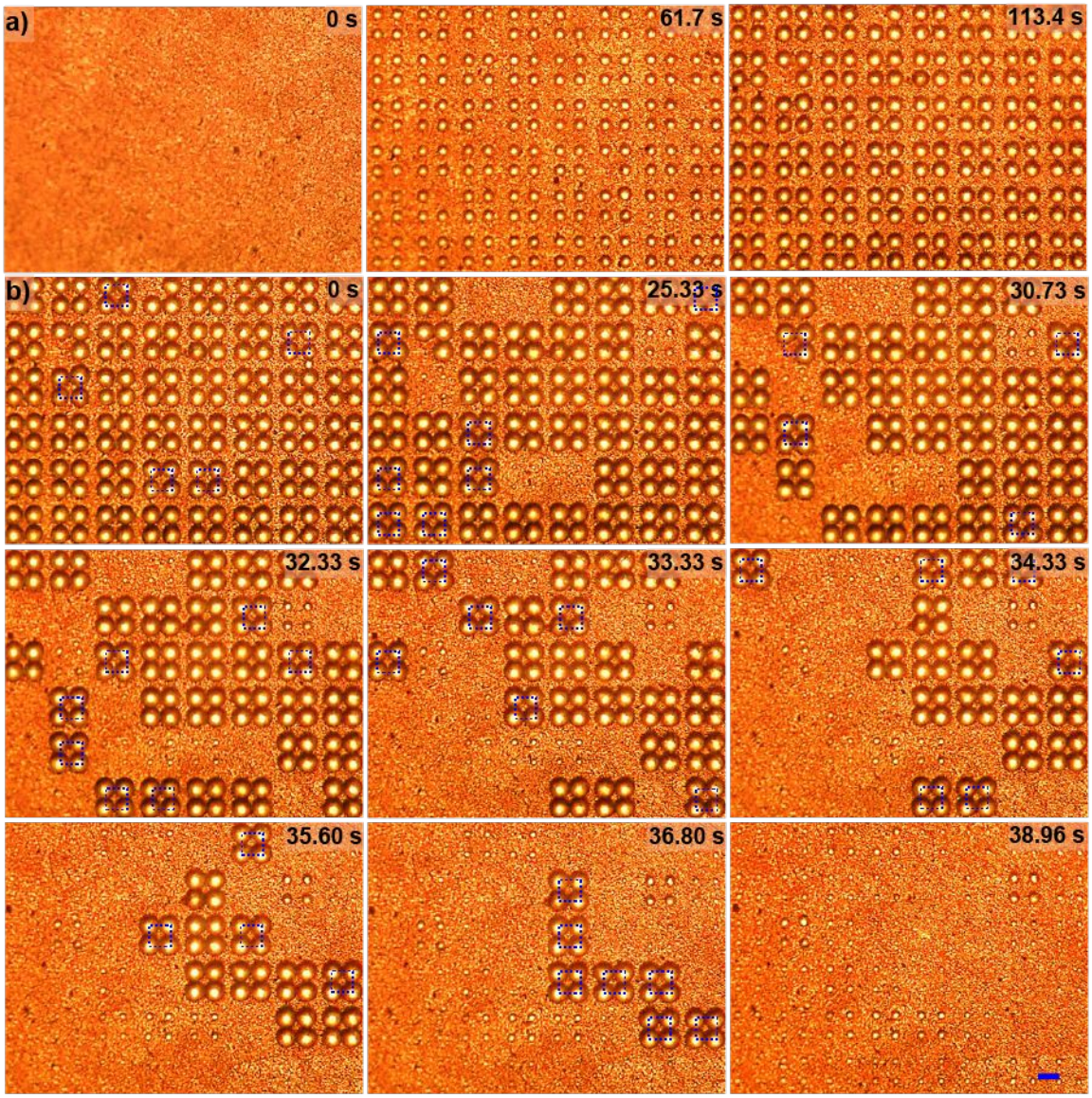

Figure S4. Large-area optical images are given to present the confined growth (a) and controlled coalescence/self-ejection (b) details of condensate on the heterogeneously-patterned surface with $N = 4$, $D = 2$ μm, $P = 20$ μm, $L = 26$ μm. Here, "0 s" labeling in the panel of **a** and **b** refers to the moment of condensation beginning and the moment before the first coalescence of "in-site" condensate microdrops, respectively. Such heterogeneous pattern can simultaneously realize the confined growth, coalescence and self-ejection.

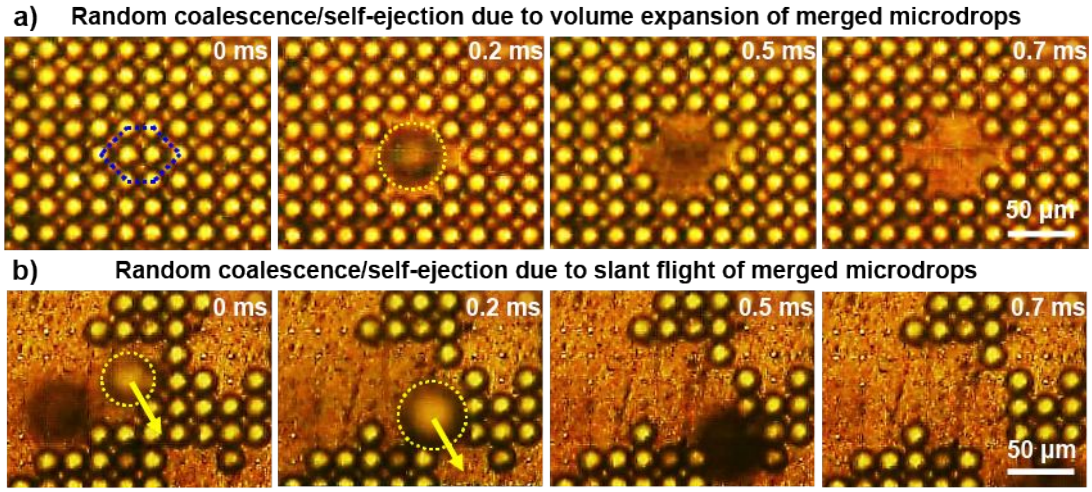

Figure S5. Proofs of two distinct random coalescence/self-ejection ways on the homogeneously-patterned surface (*e.g.*, N = 4, D = 2 μm and L = P = 20 μm). a) Representative time-lapsed optical images showing that the coalescence/ejection event is uncontrolled and triggered by the deformation of microdrops during their coalescence process, which can randomly touch adjacent microdrops. b) Time-lapsed optical images showing that random coalescence/ejection events can also be triggered by self-ejected microdrop, which can randomly touch and take away adjacent microdrops along their flight trajectory. In principle, these two random coalescence/self-ejection mechanisms can occur on all sample surfaces except for those optimized heterogeneously-patterned surfaces with synergistic controlled self-removal function of patterned condensate microdrops.